

Seismological Research Letters

This copy is for distribution only by
the authors of the article and their institutions
in accordance with the Open Access Policy of the
Seismological Society of America.

For more information see the publications section
of the SSA website at www.seismosoc.org



THE SEISMOLOGICAL SOCIETY OF AMERICA
400 Evelyn Ave., Suite 201
Albany, CA 94706-1375
(510) 525-5474; FAX (510) 525-7204
www.seismosoc.org

The 24 January 2013 M_L 4.4 Earthquake near Paradox, Colorado, and Its Relation to Deep Well Injection

**by Lisa V. Block, Christopher K. Wood, William L. Yeck,
and Vanessa M. King**

INTRODUCTION

A local magnitude (M_L) 4.4 earthquake occurred near the town of Paradox, in western Colorado, on 24 January 2013, at 4:46:39 UTC time (23 January 2013, at 9:46:39 p.m. local time) and was strongly felt in nearby communities. Earthquakes this large are infrequent in the region. A search of regional earthquake databases yields just nine previous earthquakes of magnitude 3.5 or larger recorded since 1985, and occurring within 200 km of the January 2013 earthquake epicenter (Fig. 1). Of these nine earthquakes, the epicenters of four are within several kilometers of an active brine deep injection well, and, based on their timing and location, we interpret them to be induced by injection operations.

The 24 January 2013 earthquake was recorded by the Paradox Valley Seismic Network (PVSN), a local 20-station surface array of broadband three-component seismometers installed to monitor earthquakes induced by fluid injection at the Paradox Valley Unit (PVU) deep brine disposal well. PVSN has been continuously operated in various configurations since 1985, including a six-year pre-injection baseline period. Ground motions from the January 2013 earthquake were also recorded by strong-motion instruments at three free-field sites located between 5 and 12 km from the epicenter. In this article, we provide analyses of the January 2013 event based on data from the local seismic network and strong-motion instruments. We compare the event to earthquakes recorded previously in this area, and we compare the recorded strong ground motions to estimates obtained using several empirical ground-motion prediction equations.

DESCRIPTION OF THE EARTHQUAKE

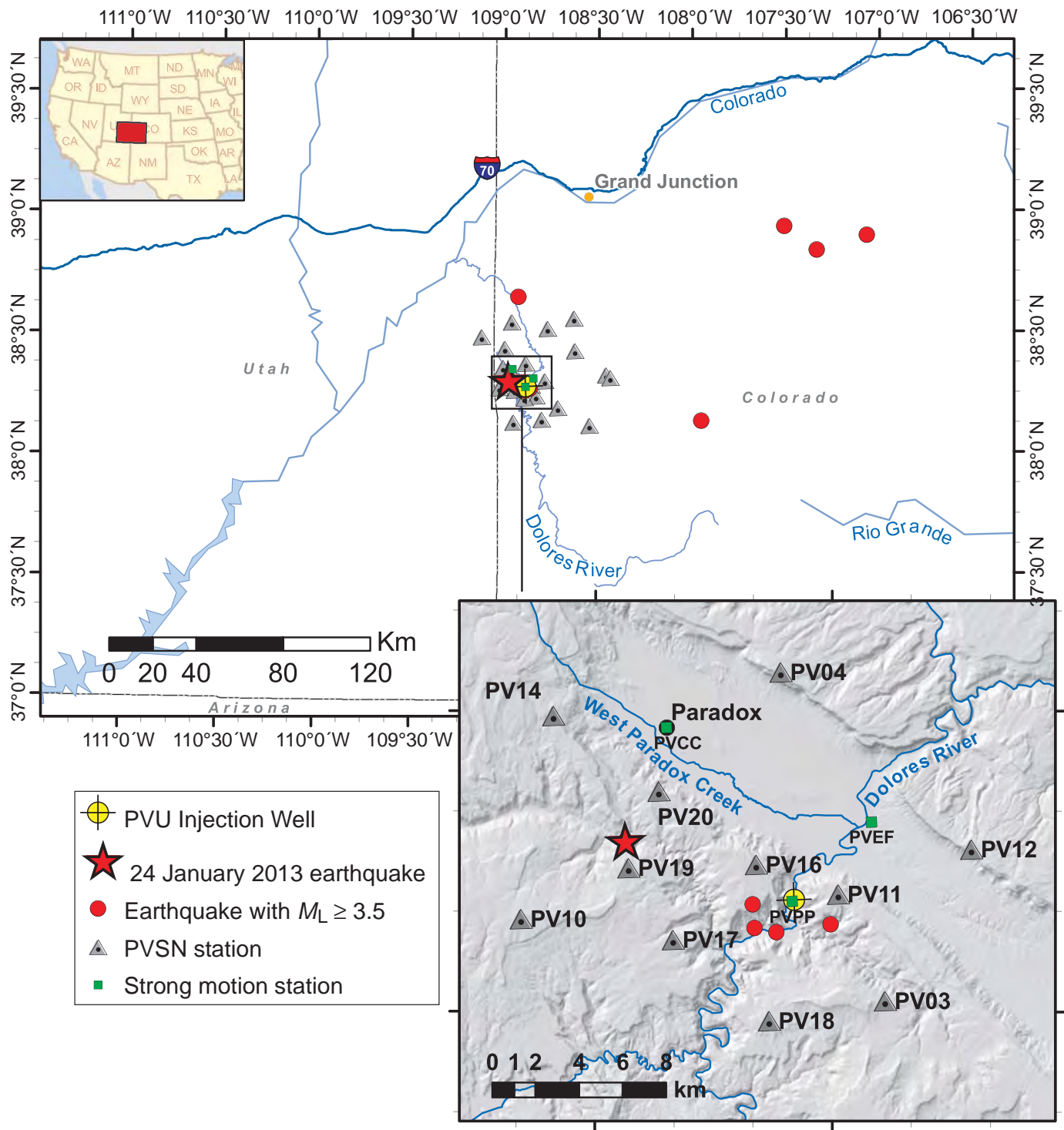
The January 2013 earthquake occurred 8.2 km northwest of the PVU injection well and 5.6 km southwest of the town of Paradox, Colorado (Fig. 1). The epicenter is within the boundary of the PVSN and less than 1.5 km from the nearest seismic station. We computed a hypocenter for the event using P - and S -wave arrival times from PVSN and a local 3D velocity model we developed previously. The computed epicenter is at latitude 38.3209° N, longitude 108.9841° W, and the focal depth is 4.4 km below the local ground surface.

We calculated a moment magnitude of M_w 4.0 from the displacement spectra at long periods of P and S waves at all PVSN broadband stations having good-quality data. Although the seismic waveforms from the PVSN stations closest to the epicenter were clipped, and therefore not usable in this analysis, many of the more distant stations provided useful data. Assuming a simple Brune (1970, 1971) circular rupture model, we also determined a static stress drop of 20 bars and rupture radius of 0.6 km. The moment magnitude we computed is consistent with magnitudes computed by the U.S. Geological Survey's (USGS) National Earthquake Information Center using data from regional seismic stations, which include: moment magnitude M_w 3.9, local magnitude M_L 4.4, and body-wave magnitude m_b 3.8 (Harley Benz, personal comm., 2013).

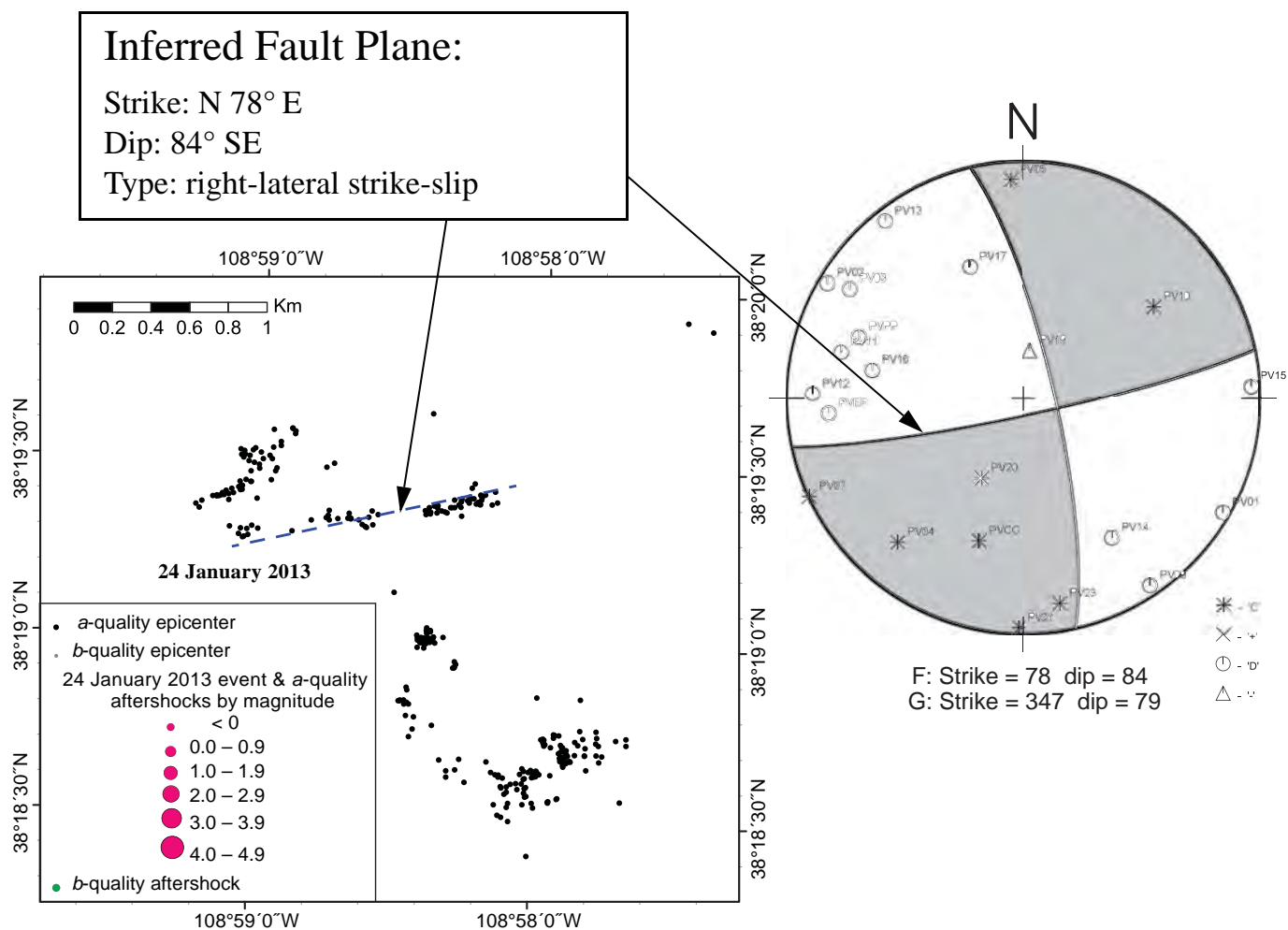
First-motion analysis of data from PVSN stations indicates that the earthquake was produced by strike-slip rupture of either of two conjugate steeply dipping fault planes: (1) a fault striking N13°W, and dipping 79° NE; or (2) a fault striking N78°E, and dipping 84° SE. The estimated directions of compression (P axis) and extension (T axis) are N58°W and N32°E, respectively. Epicenters of past events and aftershocks of the January 2013 earthquake suggest that the second conjugate fault orientation, N78°E, is the rupture plane. Based on precise relative locations, epicenters of these events form a 1.5 km long linear zone oriented approximately N78°E, consistent with the east-northeast-striking conjugate fault plane. The January 2013 earthquake and its aftershocks occurred within this linear zone (Fig. 2).

RELATION TO PARADOX VALLEY UNIT FLUID INJECTION

Available data indicate that the January 2013 earthquake was induced by long-term PVU fluid injection. The earthquake occurred within a persistent cluster of induced seismicity located 6–8 km northwest of the injection well (Fig. 3). This cluster has been seismically active since mid-1997, approximately one year after the start of long-term fluid injection. The focal depth of the January 2013 earthquake is approximately 4.1 km below the elevation of the injection wellhead, which is consistent both with the depths of previously induced events and with the depth range of the subhorizontal injection target formations



▲ **Figure 1.** Epicenters of M_L 3.5+ earthquakes recorded in the vicinity of Paradox, Colorado, since 1985. The earthquake epicenters shown were taken from the following sources: Reclamation’s Paradox Valley Seismic Network (PVSN) catalog, the U.S. Geological Survey (USGS) Advanced National Seismic System (ANSS) catalog (<http://earthquake.usgs.gov/monitoring/anss>; last accessed 5 February 2013), the USGS National Earthquake Information Center Preliminary Determination of Epicenters (NEIC-PDE) Bulletin (<http://earthquake.usgs.gov/research/data/pde.php>; last accessed 5 February 2013), and the University of Utah Seismograph Stations (UUS) catalog (<http://www.quake.utah.edu>; last accessed 5 February 2013).



▲ **Figure 2.** First motions and computed focal mechanism of the January 2013 event, and map showing the distribution of previously induced earthquakes in the vicinity of the January 2013 event (*a*-quality epicenters, black dots; *b*-quality epicenters, gray dots) and the locations of the January 2013 earthquake and aftershocks observed through July 2013 (*a*-quality epicenters, magenta circles; *b*-quality epicenters, green circles). Except for the main event, the *a*-quality epicenters were determined using a relative location routine and precise time differences from waveform cross correlations. The main event was tied into the relative location using time differences from high-quality manual arrival-time picks. The *b*-quality epicenters were computed using manual arrival-time picks and a local 3D velocity model.

(Fig. 4), and is significantly shallower than naturally occurring seismicity in the region.

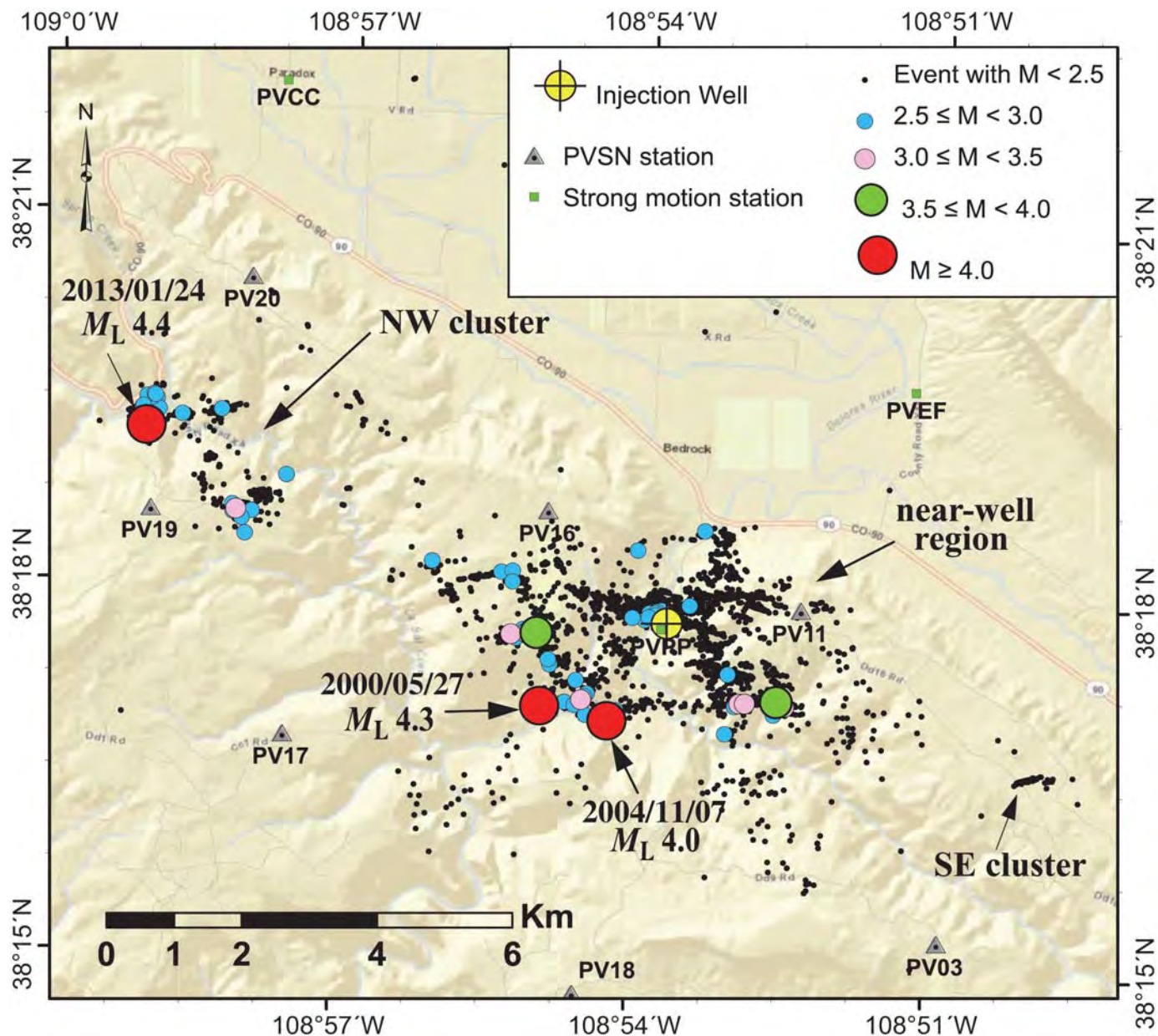
In the following sections, we provide background information about the PVU injection, seismic monitoring, local geology, and historical patterns of PVU-induced seismicity, and we compare characteristics of the January 2013 event to those of previous PVU-induced earthquakes.

PVU Injection and Seismic Monitoring

The Bureau of Reclamation's PVU has been disposing of brine in a single deep injection well almost continuously since mid-1996. A series of injection tests conducted between 1991 and 1995 preceded long-term injection. The target injection formation is characterized by relatively low porosity (< 10%) and low permeability (< 10 mD). Injection is carried out using constant-volume pumps, and the observed wellhead pressures of

up to 35 MPa represent the response of the formation to the applied fluid flows. Calculated downhole injection pressures at the depth of the target formation are as high as 84 MPa, which is above the estimated fracture-propagation pressure of approximately 70 MPa. To date, 7.6 million cubic meters of fluid have been injected.

The PVSN has been an integral part of PVU throughout the history of the project. The objectives of the network were to determine pre-injection seismicity levels in the area, and to provide continuous monitoring capability of induced earthquakes once injection operations began. Installation of what was originally a 10-station short-period network began in 1983, with the network becoming continuously operational by 1985. PVSN has been expanded and updated over the years, and the network currently consists of 20 three-component broadband surface seismometers and three strong-motion accelerographs.



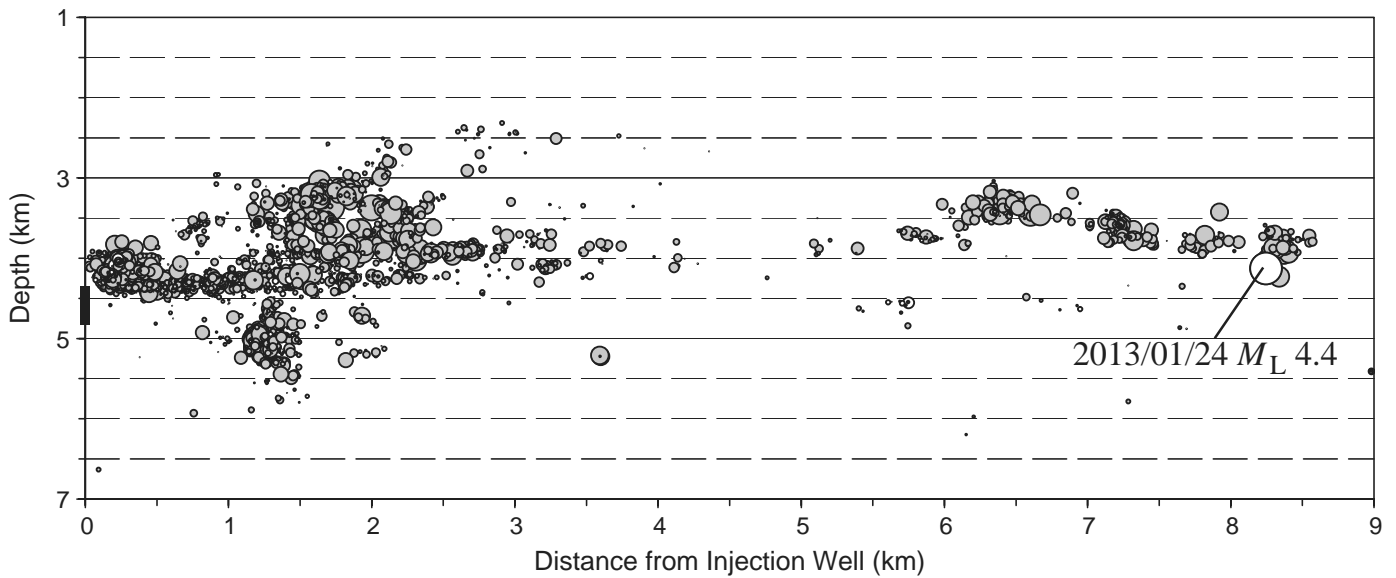
▲ **Figure 3.** PVU-induced seismicity in the near-well region (within 5 km of the injection well) and northwest cluster (6–8 km northwest of the well). The three largest PVU-induced earthquakes are shown in red and labeled with their dates and magnitudes.

PVU is a component of the Colorado River Basin Salinity Control Program, an effort to improve water quality in the Colorado River system. PVU intercepts highly saline groundwater flows that would otherwise enter the Dolores River, a tributary of the Colorado River, and disposes of the brine by deep-well injection. The U.S. Department of the Interior, Bureau of Reclamation (Reclamation) operates the PVU brine extraction, injection, and seismic monitoring programs.

Local Geology

Paradox Valley is located in the Paradox fold and fault belt and was formed by the collapse of a northwest-trending diapiric

salt-cored anticline (Cater, 1970; Gutierrez, 2004; Trudgill, 2011). The PVU injection well is located on the southwest flank of the salt anticline (Fig. 5). The well penetrates Triassic through Cambrian sedimentary rock layers and granitic Precambrian basement. With the exception of the Paradox Formation, which consists primarily of highly deformed salt layers, the geologic units are generally subhorizontal. The basement and overlying sedimentary layers are offset by a series of northwest-trending high-angle normal faults, which result in an overall deepening of the rock units toward the northeast (Fig. 5). These deep faults do not extend to the ground surface. Their locations have been mapped using deep seismic reflection



▲ **Figure 4.** PVU-induced earthquakes having well-constrained relative hypocenters, plotted as a function of distance from the PVU injection well and depth (relative to the ground-surface elevation at the wellhead). Each circle represents a single earthquake, with the width of the circle scaled by the event magnitude. The January 2013 earthquake is labeled, and the perforated interval in the injection well (4.3–4.8 km depth) is indicated by the thick vertical line on the left side of the graph.

and well-log data, but are only approximately known (Block *et al.*, 2012; King *et al.*, submitted).

Based on interpretation of regional core and log data, the Mississippian Leadville carbonate was selected as the primary injection formation. This unit has a thickness of 127 m at the PVU injection well site. Some of the underlying early to mid-Paleozoic limestone and sandstone units and the Precambrian basement were considered supplemental reservoirs. The well casing was perforated in several intervals between the top of the Leadville Formation (4.3 km depth) and the bottom of the borehole (4.8 km depth). The overlying Paradox Salt Formation acts as a confining layer.

Historical Seismicity Patterns

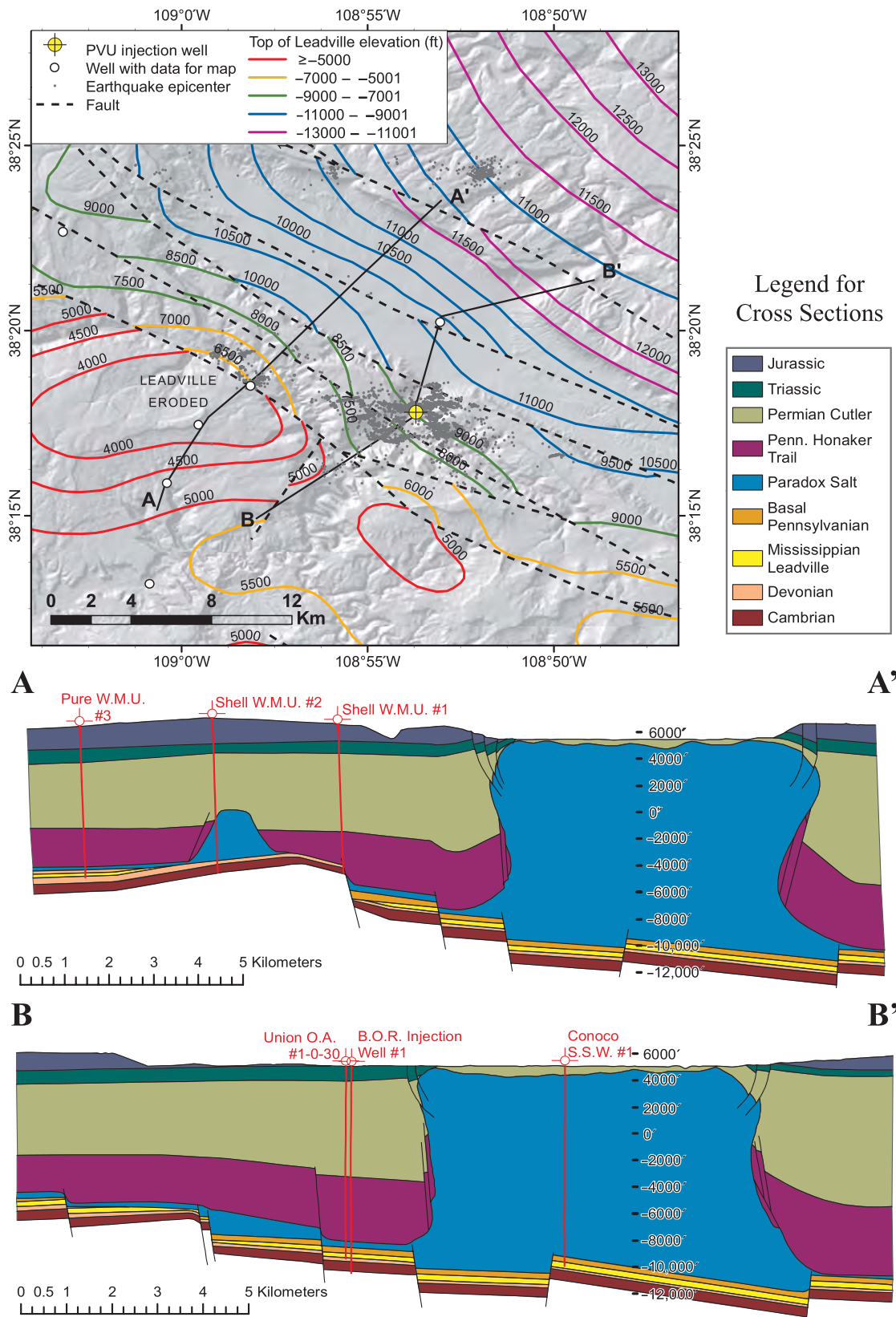
PVSN has recorded more than 5900 shallow earthquakes in the vicinity of Paradox Valley since injection tests began in 1991. In contrast, a review of historical PVSN data files indicates only one local earthquake for the six years prior to injection (1985–1990), and it occurred about 19 km from the PVU injection well, at an estimated depth of 15 km. The vast majority of earthquakes recorded since the start of injection have focal depths between 2.5 and 6.5 km below the injection wellhead elevation. These depths are consistent with the depth range of injection (4.3–4.8 km). In addition, the events are substantially shallower than the few naturally occurring tectonic earthquakes that have been recorded in the area, which have focal depths exceeding 10 km. Although most earthquakes observed since the start of injection have occurred within 4 km of the injection well, shallow seismicity has also occurred as far as 17 km from the well.

Previously published analyses of the PVSN earthquake data focused on events occurring within 9 km of the injection well

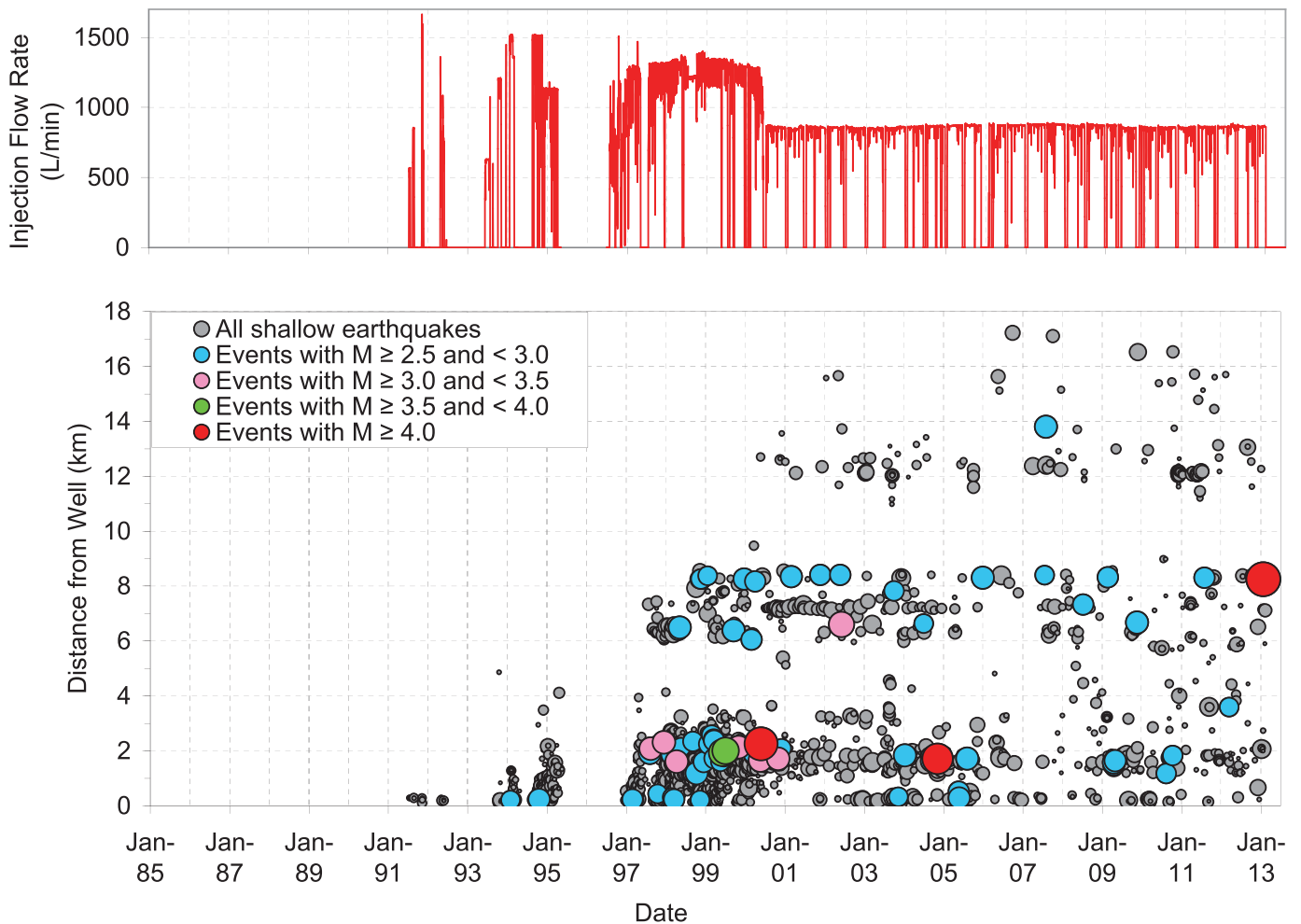
(Ake *et al.*, 2005; Mahrer *et al.*, 2005). Analyses of earthquakes occurring at greater distances from the well and their potential relationship to PVU fluid injection had been limited for several reasons. These included errors in the earthquake catalog (such as incorrect event classification and location), relatively large uncertainties in depth estimates for distant earthquakes, and an incomplete understanding of variations in PVSN’s event detection capability over time.

Over the last several years, we completed comprehensive re-analysis of the historical PVSN data and implemented improvements in seismic monitoring that have allowed us to extend our interpretation of PVSN-recorded seismicity to distances up to approximately 20 km from the injection well. This work included retrieval of unprocessed data from computer backup tapes, automatic and manual reprocessing of thousands of events, evaluation of temporal variations in PVSN’s event detection capabilities, upgrade of existing PVSN seismic stations to three-component broadband digital instrumentation, and installation of six new stations to improve coverage. The network improvements resulted in more accurate hypocenter estimates for earthquakes occurring more than a few kilometers from the injection well. Furthermore, we were able to improve the hypocenter estimates of older earthquakes by relocating them relative to recent events recorded with the improved network geometry. As a culmination of these efforts, we produced a revised local earthquake catalog that has significantly improved our knowledge of the spatiotemporal pattern of seismicity in the Paradox Valley region since injection began.

The revised PVSN local earthquake catalog provides clear evidence that the zone of shallow seismicity has continued to



▲ **Figure 5.** Contour map of the top of the Leadville Formation and geologic cross sections perpendicular to Paradox Valley. These geologic interpretations are based on analysis of sparse seismic reflection and well-log data, and only provide a basic understanding of the deep geologic structure. The geologic model presented here is based on the work of Bremkamp and Harr (1988) and is described in more detail in Block et al. (2012) and King et al. (submitted).

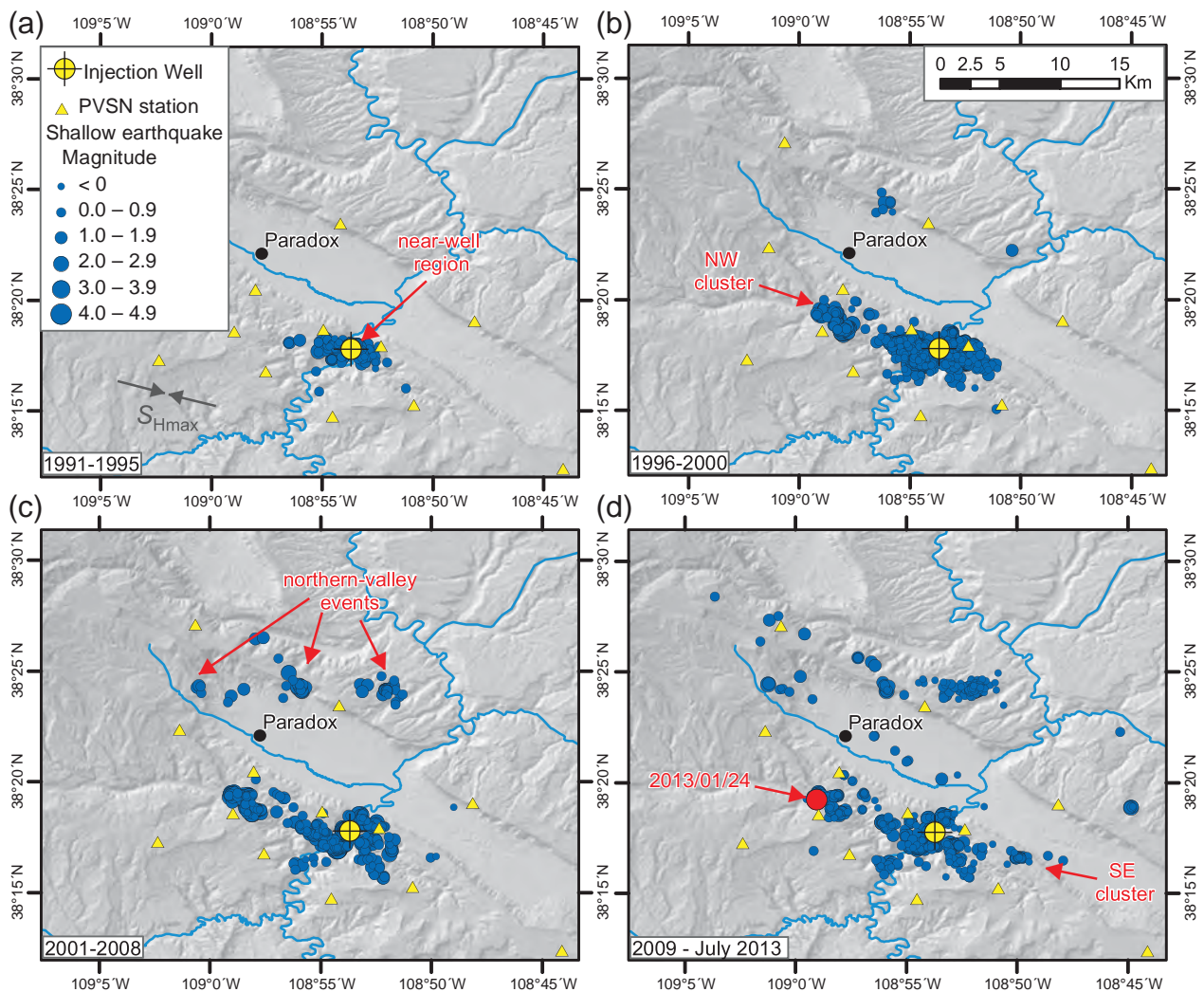


▲ **Figure 6.** Scatter plot of earthquakes having $M \geq 0.5$ and locating less than 8.5 km deep (relative to the ground-surface elevation at the injection wellhead), plotted as a function of date and distance from the PVU injection well (lower plot). Each circle represents a single earthquake, with the width of the circle scaled by the event magnitude. The upper plot shows the daily average injection flow rate over the same time period.

spread from an initial locus about the PVU injection well since injection began in 1991 (Fig. 6). Within four days after the start of the first injection test in July 1991, earthquakes were detected in the immediate vicinity of the injection well. As injection continued, earthquakes were detected at progressively increasing radial distances, and, by 2002, shallow earthquakes were occurring nearly 16 km from the well (Fig. 6). We interpret the majority of the shallow earthquakes recorded since 1991 as being induced by PVU fluid injection. This interpretation is based on the nearly complete lack of seismicity detected during six years of pre-injection monitoring, the close correspondence of the depths of the earthquakes and that of injection, and the spatiotemporal evolution of the seismicity distribution since injection began (see Fig. 6).

Several distinct groups, or clusters, of induced seismicity have developed over the history of PVU injection. By the end of the injection tests in 1995, earthquakes were occurring 3–4 km from the well (Fig. 7a). We refer to this area of induced

seismicity immediately surrounding the injection well as the near-well region. In 1997, about one year after the start of long-term injection, earthquakes began occurring 6–8 km northwest of the injection well (Fig. 7b). We identify this group of induced seismicity as the northwest cluster. The epicenter of the January 2013 M_L 4.4 earthquake is within this group of events (Fig. 7d). In mid-2000, PVSN first detected earthquakes 12–14 km from the injection well, along the northern edge of Paradox Valley (Fig. 7b). Several distinct clusters of earthquakes have occurred along the northern edges of the valley since 2000 (Fig. 7c,d). We refer to the earthquakes in all of these groups as northern-valley events. An earthquake was first detected about 6 km southeast of the injection well in 2004 (Fig. 7c), but the seismicity rate in this area markedly increased beginning in 2010 (Fig. 7d). We identify this compact group of earthquakes as the southeast cluster. In recent years, a few isolated earthquakes have been detected in previously aseismic areas, including beneath central Paradox Valley (Fig. 7d).



▲ **Figure 7.** Maps showing the spatial distribution of shallow seismicity recorded in the Paradox Valley area over time: (a) injection tests, 1991–1995; (b) continuous injection, 1996–2000; (c) continuous injection, 2001–2008; and (d) continuous injection, 2009–July 2013. All detected earthquakes locating less than 8.5 km deep (relative to the ground-surface elevation at the injection wellhead) are included. The paired black arrows in map (a) indicate the interpreted direction of regional maximum horizontal compressive stress (Ake *et al.*, 2005).

COMPARISON OF THE JANUARY 2013 EARTHQUAKE TO PREVIOUS PVU-INDUCED EARTHQUAKES

Magnitude and Distance from the Well

For consistency, we use the local magnitude scale M_L in comparing the size of the January 2013 earthquake to historical PVU-induced events because M_L determinations are available for all events with $M_L \geq 3.5$. Moment magnitude estimates are available for only a subset of pre-2011 events. Prior to 2013, the largest PVU-induced earthquake was an M_L 4.3 event, which occurred on 27 May 2000. The January 2013 earthquake, with M_L 4.4, is slightly larger than the May 2000 event, making it the largest PVU-induced earthquake to date. A comparison of the local and moment magnitudes of the three largest PVU-induced earthquakes recorded to date is provided in Table 1.

The January 2013 event is the only induced earthquake with M_L 3.5 or greater (M_L 3.5+) to occur at a distance

greater than about 2 km from the injection well. The previous four PVU-induced M_L 3.5+ events occurred in a narrow band between 1.6 and 2.2 km from the injection well (Fig. 3). At a distance of 8.2 km from the injection well, the January 2013 earthquake epicenter is nearly four times farther from the well than that of any previous PVU-induced earthquake of comparable magnitude. In addition, the January 2013 earthquake is only the second earthquake with duration magnitude of M_D 3.0 or greater to occur more than about 2 km from the injection well. The other M_D 3.0+ earthquake at a relatively large radial distance is a M_D 3.3 event that occurred within the northwest cluster in June 2002, at a distance of about 6.6 km from the well (Fig. 3).

Focal Mechanism

The observed strike-slip mechanism of the January 2013 earthquake (Fig. 2) is consistent with mechanisms of previous PVU-induced earthquakes. Ake *et al.* (2005) found that strike-slip

Table 1
Comparison of Local and Moment Magnitudes for the Three Largest PVU-Induced Earthquakes

Earthquake Date (yyyy/mm/dd) (UTC)	Local Magnitude (M_L)	Moment Magnitude (M_w)
2000/05/27	4.3 (UUSS)	3.8 (SLU)
2004/11/7	4.0 (USGS)	3.6 (SLU)
2013/01/24	4.4 (USGS)	3.9 (USGS) 4.0 (USBR)

The source for each magnitude estimate is given in parentheses: UUSS, University of Utah; SLU, Saint Louis University; USGS, U. S. Geological Survey; USBR, Bureau of Reclamation.

mechanisms accounted for 89% of 1345 well-determined focal mechanisms of events in the near-well region, and they interpreted 86% of the strike-slip mechanisms they studied to have fault-plane azimuths of N86°E. The east-northeasterly orientation of the interpreted fault plane of the January 2013 earthquake, N78°E, is consistent with these earlier findings. The estimated direction of compression (P axis) for the January event, N58°W, is roughly consistent with the analyses of [Ake et al. \(2005\)](#), who determined a mean P axis azimuth of N64°W–N67°W.

Nearby Seismicity

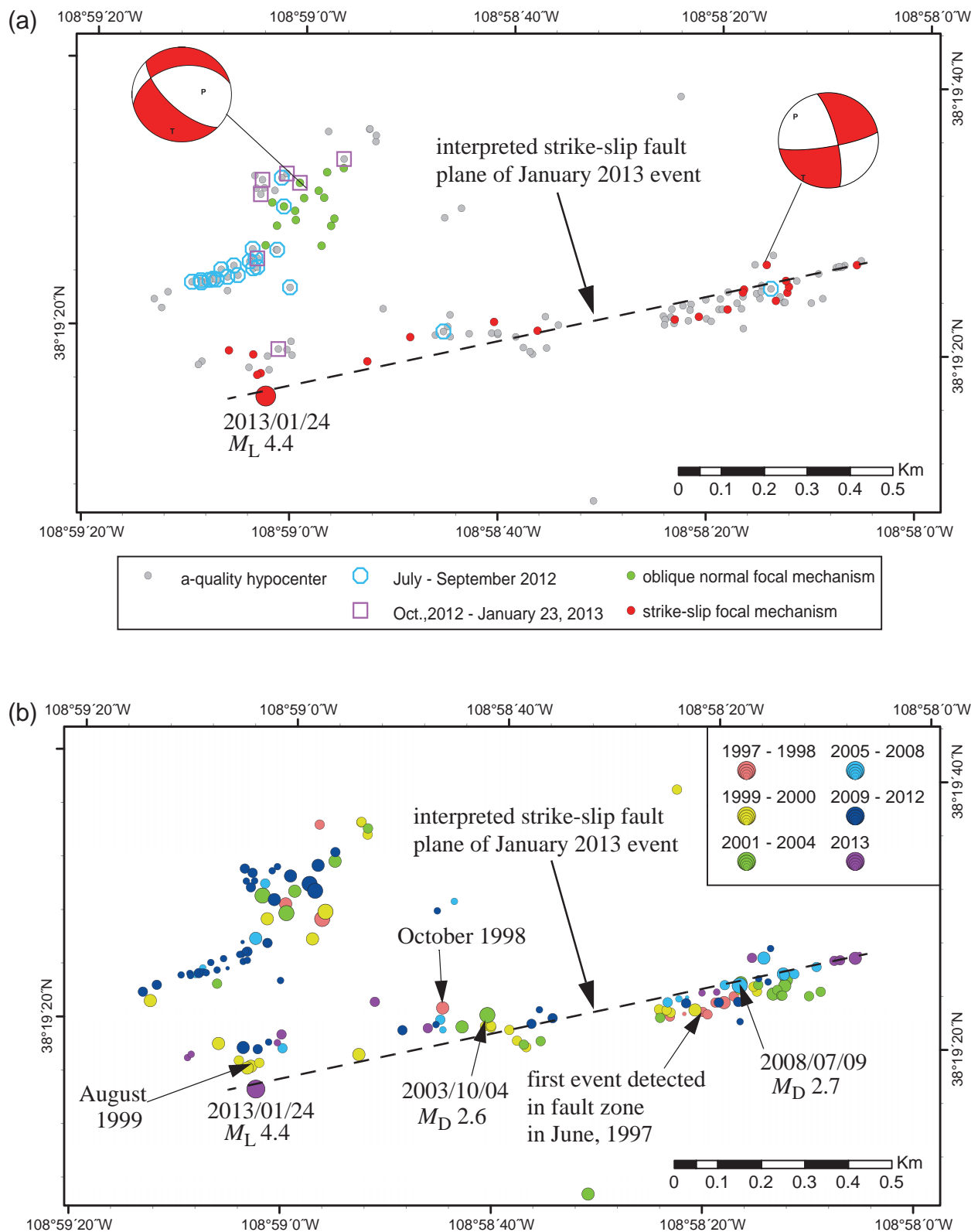
In the six months prior to the January 2013 event, PVSN recorded about 30 induced seismic events within one kilometer of the mainshock epicenter. These foreshocks had duration magnitudes less than M_D 2.0, with most having $M_D \leq 1.0$. We did not observe any increase in maximum event magnitude or any substantial change in the rate of $M_D \geq 0.5$ events in the weeks or months prior to the January 2013 earthquake. In contrast, a large increase in the rate of detected events with magnitude M_D 0.0–0.5 occurred during the third quarter of 2012, with five times more M_D 0.0–0.5 events recorded during this three-month period than in any previous quarter. However, the baseline period to determine seismicity rates of M_D 0.0–0.5 events was only about a year and a half at the time of the January 2013 event, because events this small were not reliably detected in this area until after the installation of two additional nearby seismic stations in July 2011. Rates of M_D 0.0–0.5 events returned to normal levels during the fourth quarter of 2012. Hence, we have limited data to indicate whether the observed increased rate of M_D 0.0–0.5 events a few months prior to the January 2013 earthquake is anomalous.

We found that earthquakes in the vicinity of the January 2013 event can be grouped into two distinct faulting types, based on an analysis of 35 events with well-constrained relative hypocenters and focal mechanisms: (1) strike-slip faulting consistent with that of the January 2013 earthquake, and (2) oblique normal faulting. The average strike-slip focal mechanism from 20 events is N76°E, dip 76°SE, with about 5° standard deviations of strike and dip. The average oblique normal mechanism from 15 events is: (a) strike N42°W, dip 71°SW, or (b) strike N77°E, dip 35° NW, with standard deviations of strike and dip less than 7°. Epicenters of these earthquakes are plotted by focal mechanism type in Figure 8a. All analyzed events with strike-slip mechanisms are distributed

along the inferred east-northeast-trending fault segment interpreted to have ruptured during the January 2013 earthquake. In contrast, all events with the oblique-normal mechanism form a tightly spaced cluster about 250–450 m north of the strike-slip fault plane. Most of the foreshocks detected in the six months prior to the January 2013 earthquake occurred near this cluster, and relatively few foreshocks occurred near the interpreted mainshock fault plane (Fig. 8a, squares and octagons). Most of the foreshocks, however, do not have sufficiently good data to compute robust focal mechanisms because of their small magnitude.

The area surrounding the inferred rupture of the January 2013 earthquake has been seismically active since at least June 1997, when PVSN recorded a cluster of earthquakes near the eastern end of the fault segment (Fig. 8b). In October 1998, an earthquake was detected near the center of the fault segment, approximately 500–700 m west of the initial cluster of events. By August 1999, seismicity was occurring near the western end of the fault segment, to within 100 m of the January 2013 event epicenter (Fig. 8b). The seismicity pattern delineating the western end of the fault segment has not grown in size since 2000, suggesting that the segment is truncated in this direction, either by a major northwest-trending normal fault or by pinch-out of the primary injection target formation due to erosion ([Block et al., 2012](#); [King et al., submitted](#)). The seismicity pattern delineating the eastern limit of the fault segment has continued to expand slowly, and several aftershocks of the January 2013 event have extended seismicity on the fault segment to the east by about 100 m.

The entire fault segment, as inferred from pre-2013 seismicity, appears to have ruptured during the January 2013 earthquake. Aftershocks of the January 2013 earthquake occur near both ends of the pre-2013 seismicity zone (Fig. 2), and the inferred fault segment length determined from the seismicity distribution is consistent with the rupture dimension expected for the moment magnitude of the January 2013 earthquake. Using a simple circular crack model ([Brune, 1970, 1971](#); [Kanamori and Anderson, 1975](#)) with crack radius equal to one half of the fault segment length indicated by the pre-2013 epicenters (1.4 km), and a static stress drop equivalent to that determined for the January 2013 earthquake (20 bars), we obtain a moment magnitude of M_w 4.1 for rupture of the entire fault segment. This value is very close to the Reclamation-computed M_w of 4.0 for the January 2013 earthquake and only slightly larger than the USGS M_w estimate of 3.9. Changing



▲ **Figure 8.** Epicenters of earthquakes with well-constrained relative locations in the near vicinity of the January 2013 M_L 4.4 earthquake. (a) Earthquakes having similar strike-slip focal mechanisms are indicated by the filled red circles, and those having similar oblique normal focal mechanisms are indicated by the filled green circles. A typical focal sphere plot for each type of mechanism is shown. Gray circles indicate events without well-defined focal mechanisms. Earthquakes occurring during the six-month period before the January 2013 event are identified by the open squares and octagons, as indicated in the legend. (b) Earthquakes color-coded by year of occurrence and with symbol size scaled by event magnitude.

the assumed stress drop by a factor of 2 results in a change of $0.2 M_w$ units, and therefore these results are relatively insensitive to small changes in the assumed stress-drop value.

Although small earthquakes have occurred since 1999–2000 along most of the inferred fault segment that ruptured in January 2013, an additional 13 years elapsed before the earthquake that finally ruptured the entire segment. Only two earlier earthquakes of $M_D \geq 2.5$ occurred on portions of this fault segment: an M_D 2.6 event occurred near the center of the fault segment in October 2003 and an M_D 2.7 event occurred near the east end of the fault segment in July 2008 (Fig. 8b). Assuming a similar stress drop as for the January 2013 earthquake (~ 20 bars), and a circular crack model, these earthquakes each ruptured less than a 300-m portion of the fault segment, or less than about 20% of the total fault-segment length. One possible explanation for the 13-year delay prior to rupture of the entire fault segment is that a pore-pressure threshold may exist that must be exceeded over most of the fault surface for rupture to propagate (Shapiro *et al.*, 2011). We have previously observed that a pore-pressure threshold may need to be reached to induce larger-magnitude earthquakes in the near-well region, based on correlation of near-well larger-magnitude earthquakes and higher injection pressures (Block and Wood, 2009, 2010). Correlation between larger-magnitude induced earthquakes and an increase in pore pressure to a threshold level over most of the fault surface has been suggested by numerical studies (Garagash and Germanovich, 2012).

STRONG GROUND MOTIONS

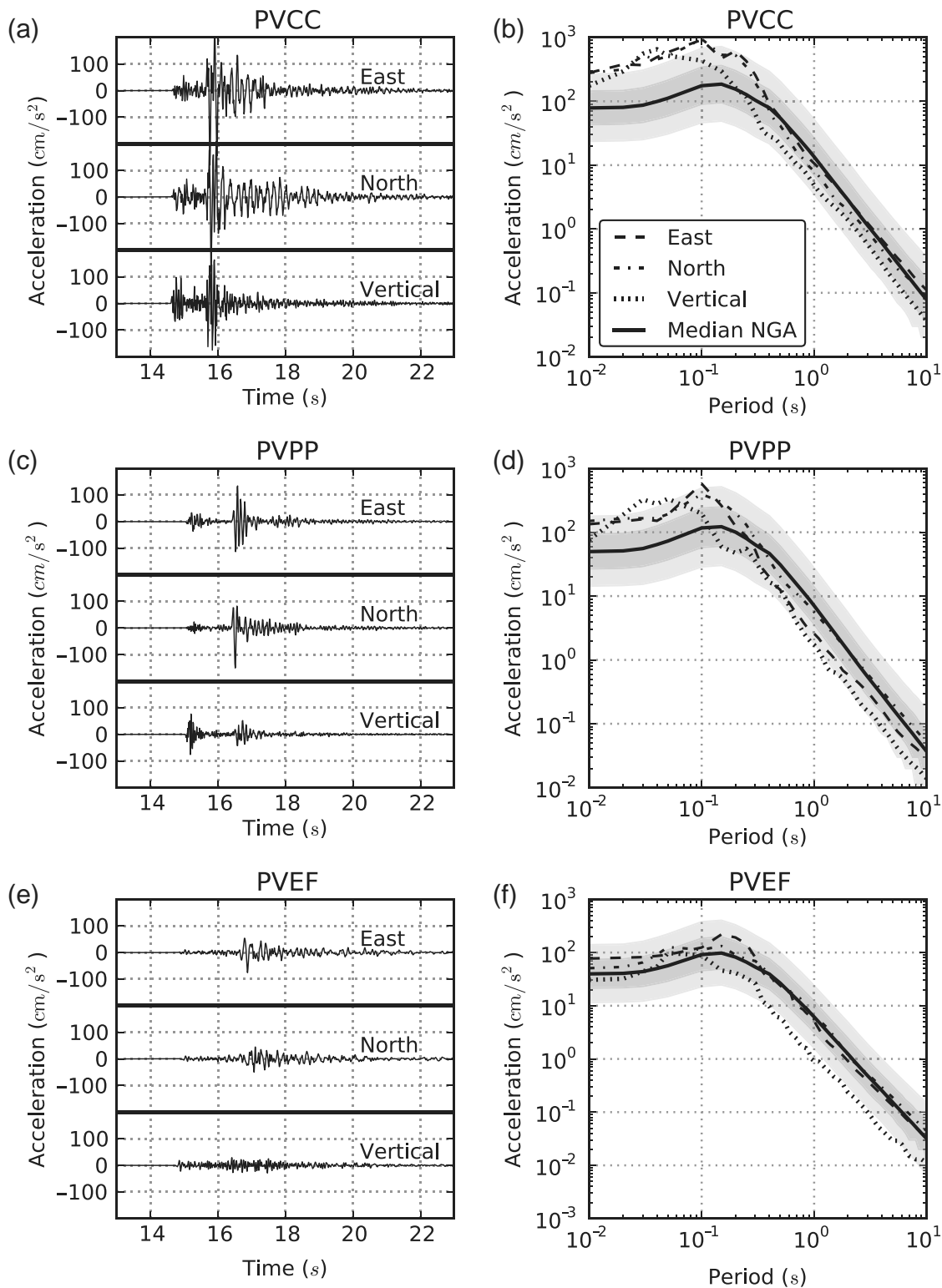
Recordings of the January 2013 earthquake were obtained from three strong-motion instruments installed by Reclamation between 1997 and 2005 to compliment the PVSN high-gain seismograph network. The strong-motion stations are located at: (1) the Paradox Community Center in the town of Paradox, Colorado (station code PVCC); (2) the PVU injection wellhead and pumping plant (station code PVPP); and (3) the PVU surface treatment facility and extraction well field (station code PVEF), as shown in Figure 1. Acceleration time histories and response spectra obtained for the January 2013 earthquake are shown in Figure 9, and a summary of derived ground-motion parameters is provided in Table 2.

Residents of northern Paradox Valley reported feeling strong shaking from the January 2013 earthquake, and the shaking was perceived as being much stronger than that experienced during previous felt earthquakes (A. Nicholas, personal comm., 2013). Press reports indicate that shaking was felt over a wide region (Silkman, 2013). The felt reports within Paradox Valley are consistent with recordings obtained from strong-motion instruments, which show peak horizontal accelerations (PHAs) of 287 cm/s^2 ($0.29g$) in the town of Paradox, 150 cm/s^2 ($0.15g$) near the PVU injection wellhead, and 75 cm/s^2 ($0.08g$) at the PVU surface treatment facility.

We evaluated whether ground motions recorded in the Paradox Valley area during the January 2013 earthquake differ

substantially from what would be expected for a tectonic earthquake of the same magnitude and at the same distances. We compared the recorded horizontal ground motions with ground motions estimated using the Next Generation Attenuation (NGA) empirical ground-motion prediction equations (Power *et al.*, 2008). We used four of the NGA equations (Abrahamson and Silva, 2008; Boore and Atkinson, 2008; Campbell and Bozorgnia, 2008; Chiou and Youngs, 2008), and used the weighted mean of the median prediction from each (and the associated $\pm 1\sigma$ and $\pm 2\sigma$ values) as simple approximations to the true median (and spread) of the combined distribution. We considered each equation equally valid for this analysis, and therefore assigned an equal weight to each. To use the NGA equations, values for the following site properties must be measured or assumed: (1) V_{S30} , defined as the time-averaged shear-wave velocity in the upper 30 m of soil, and (2) $Z_{1.0}$ and $Z_{2.5}$, defined as the depths at which shear-wave velocities reach 1.0 and 2.5 km/s, respectively. Measured values of these quantities at the strong-motion stations are unavailable, so we assumed site V_{S30} values corresponding to moderate to soft soil sites, and computed $Z_{1.0}$ and $Z_{2.5}$ values using the relations in Abrahamson and Silva (2008) and Campbell and Bozorgnia (1987), following the suggestions of Kakkamanos *et al.* (2011). Assumed properties required for the NGA relations are shown in Table 3. The NGA predictions are for a randomly oriented horizontal component of motion, but we have not corrected the data to obtain the random component; however, the results do not depend significantly on making this correction.

The observed short-period ($< \sim 0.4$ -s) spectral accelerations (SA) from the January 2013 earthquake are substantially greater than the median NGA ground-motion predictions. In Figure 9 the acceleration response spectra for the observations are compared to the median NGA predictions. For response spectral periods greater than 0.4 s, the observed SAs are consistent with the median NGA values, whereas at short periods ($< \sim 0.4$ -s), the observed SAs are much greater than the median NGA values. This effect is greatest at PVCC, but is observed at all stations. To further illustrate the difference between the predicted median NGA values and the recorded values, we computed median $\pm 1\sigma$ and median $\pm 2\sigma$ predictions, which are shown as shaded areas in Figure 9. The recorded PHA at PVCC is greater than the median $+2\sigma$ NGA prediction, and the observed PHA at PVPP is greater than the median $+1\sigma$ NGA prediction. At PVEF, the PHA is also greater than the median NGA prediction, but is less than the median $+1\sigma$ NGA prediction. In contrast, the 1.0-s SA observations at all sites are within the median $\pm 1\sigma$ NGA predictions. The distance dependence of the observed and predicted PHAs and 1.0-s SAs is shown in Figure 10, which indicates a systematic decrease in the recorded ground motions with distance. This suggests that the anomalously high observed ground motions are not due to isolated site effects. There are several potential reasons for the large short-period ground motions observed in northern Paradox Valley. These include: site effects resulting from variations in the local geologic structure, which includes a thick salt section and soft soil layer overlying bedrock;



▲ **Figure 9.** Acceleration ground-motion time histories (left) and acceleration response spectra (right) recorded by strong-motion instruments located at: (a) and (b) the community center in the town of Paradox, Colorado (PVCC), (c) and (d) the PVU injection well and pumping plant (PVPP), and (e) and (f) the PVU surface treatment facility and extraction-well field (PVEF). The time history for each component of motion at each station is plotted, offset along the y axes for clarity. The measured response spectrum for each component of motion (dashed and dotted lines) and the median spectrum computed using four Next Generation Attenuation (NGA) relations for a randomly oriented horizontal component (solid line) are shown for each station. The shaded areas indicate the median $\pm 1\sigma$ and median $\pm 2\sigma$ values of the NGA predictions.

Table 2
Peak Horizontal Accelerations (PHA) and One-Second Spectral Accelerations (1.0-s SA) for the January 2013 Earthquake Recorded by Strong-Motion Instruments Located at the Paradox Community Center (PVCC), the PVU Injection Well and Pumping Plant (PVPP), and the PVU Extraction Field Surface Treatment Facility (PVEF)

Site	Distance from Epicenter (km)	PHA (g)	1.0-s SA (g)
PVCC	5.6	0.293	0.011
PVPP	8.2	0.153	0.006
PVEF	11.3	0.077	0.006

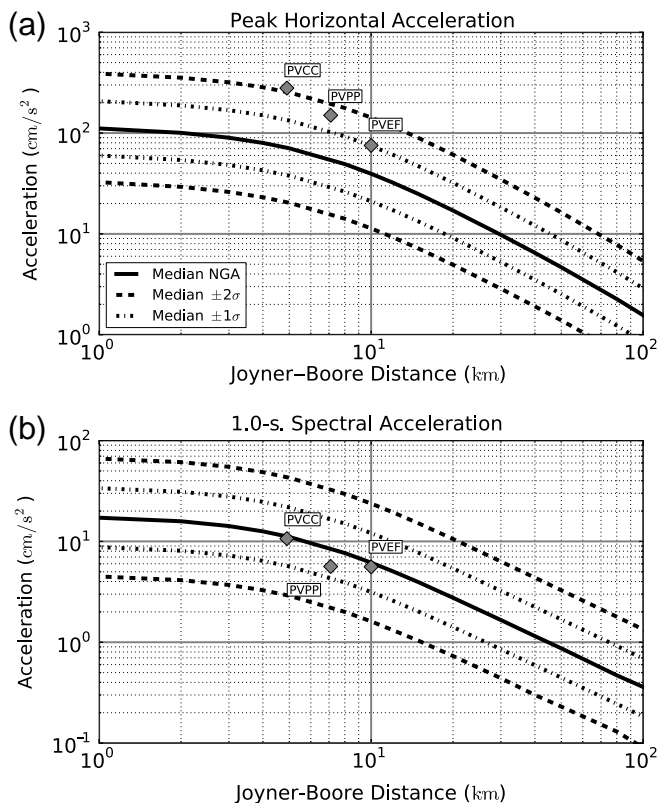
Table 3
Input Parameters Used for Estimating Ground Motions with the NGA Equations

Site	R_{JB} (km)	Z_{TOR} (km)	R_{RUPT} (km)	Dip (°)	Rake (°)	Width (km)	V_{S30} (m/s)	$Z_{1.0}$ (m)	$Z_{2.5}$ (m)
PVCC	4.9	4.0	6.3	80	5	0.6	300	330	1700
PVPP	7.1	4.0	8.1	80	5	0.6	530	170	1100
PVEF	10.0	4.0	11.8	80	5	0.6	400	220	1300

See [Kaklamanos et al. \(2011\)](#) for a description of the parameters.

unusual diffraction effects related to the diapiric salt-cored anticline; and decreased attenuation of high-frequency ground motions related to the shallow focal depth. Two of the NGA

relations used are nominally applicable only to $M \geq 5$ earthquakes (the other two are for $M \geq 4$); updates to the 2008 NGA relations expected to be published in 2014 may reduce the discrepancy between the observed and predicted ground motions.



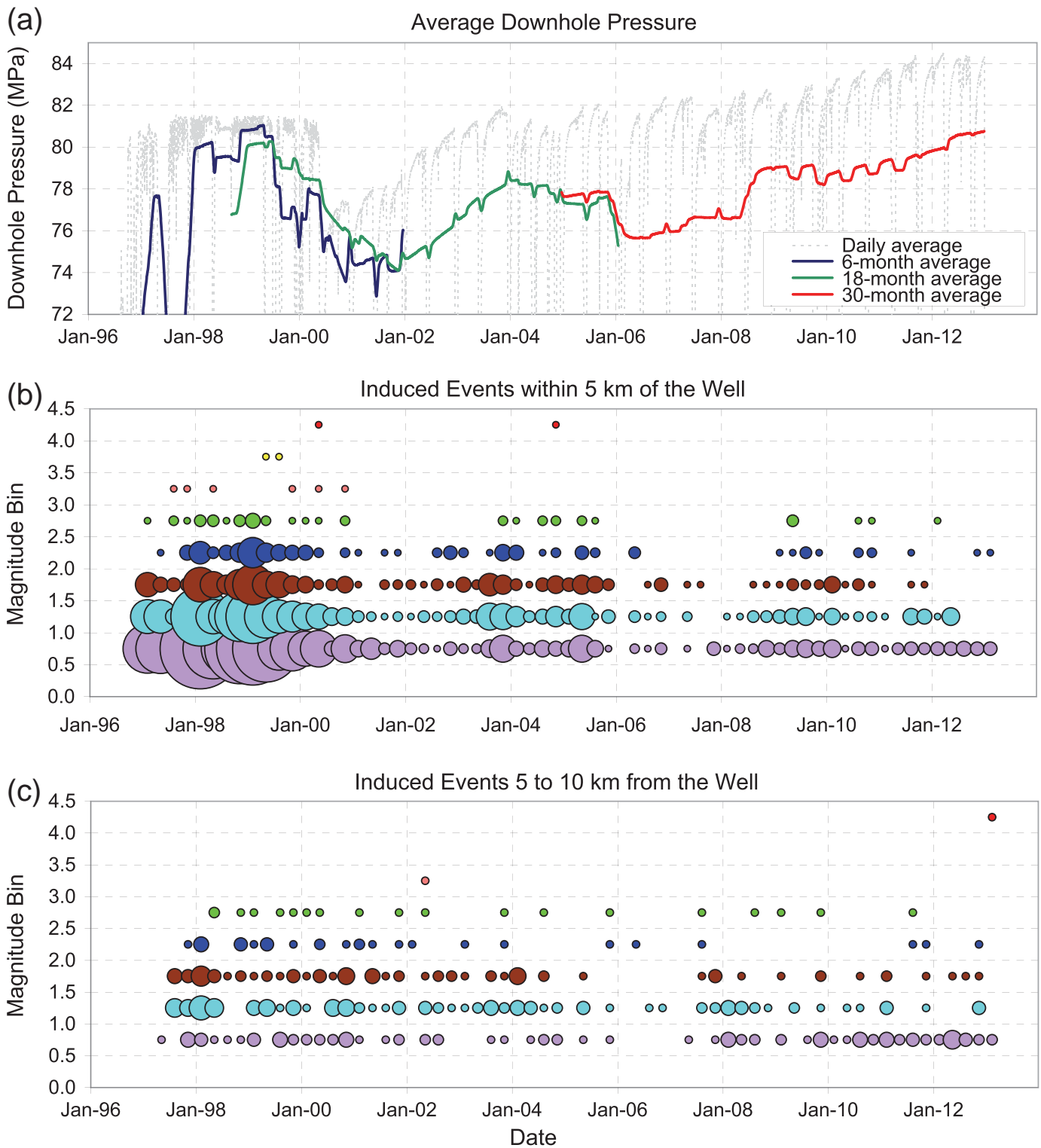
▲ **Figure 10.** Comparison of observed horizontal acceleration values (diamonds) with NGA results (lines), as a function of distance: (a) peak horizontal acceleration (b) 1.0-s spectral acceleration. The data points represent the maximum horizontal component of motion.

DISCUSSION

We interpret the shallow seismicity occurring in the vicinity of the PVU injection well as induced by fluid injection and occurring in response to a decrease in the effective normal stress on pre-existing fracture surfaces. Fracture initiation is assumed to be adequately described by a Coulomb fracture criterion ([Jaeger, 1969](#)), and the observed seismicity is interpreted to be the result of frictional failure due to shearing. Focal mechanisms analyzed to date are consistent with simple shear failure; tensile-failure events have not been recognized in the recorded data ([Ake et al., 2005](#)).

During fluid injection, the effective normal stress on pre-existing fractures may decrease as a result of increasing pore pressure, redistribution of stress (from accommodation of the injected fluid into the rock or from the occurrence of previously induced earthquakes), or cooling and shrinking of the rock matrix. The latter thermodynamic effect is important in geothermal areas, but is unlikely to be a dominant factor at PVU, except possibly in the near vicinity of the injection well. Changes in pore pressure and stress redistribution are likely the major triggering mechanisms for the earthquakes induced by fluid injection at PVU.

Simple correlation of PVU injection pressure and earthquake data suggests that pore pressure increase is a dominant factor contributing to the rate and magnitude of induced seismicity occurring within 5 km of the injection well. However, no clear correlation is observed for earthquakes occurring at greater distances, as shown in [Figure 11](#) and discussed in detail in [Block and Wood \(2009, 2010\)](#). Because we have no obser-



▲ **Figure 11.** (a) Injection downhole pressure data averaged over daily, 6-month, 18-month, and 30-month time periods, (b) occurrence of induced seismicity as a function of time and magnitude within 5 km of the injection well, and (c) at distances of 5–10 km from the well. In the seismicity plots, the area of each circle is scaled by the number of events in a given quarter-year and magnitude range. The low-seismicity rate in the smaller magnitude bins from about mid-2005 to mid-2007 in the bottom plot is believed to be due to an unusually large number of offline stations.

vation wells for measuring *in situ* pore pressures directly, we use long-term averaging of the injection pressures as a simplistic method of accounting for the time delay and amplitude modulation of pressure variations at the injection well as the pressures propagate away from the well. To correlate pressure trends with the near-well seismicity data, the pressure averaging must be done over longer time windows for later periods (Fig. 11a). The seismicity may take progressively longer to respond to changes in injection pressures both because more of the seismicity occurs at greater distances from the well during later time periods and because the size and complexity of the reservoir increases over time. Although this method is very simplistic, the general correlation between relatively high long-term average injection pressures and increased rates and magnitudes of induced earthquakes in the near-well region suggests that pore pressure affects both the rate and magnitudes of induced seismic events occurring within 5 km of the well (Fig. 11b). The same analysis, however, does not show a correlation between injection pressure and the rates and magnitudes of earthquakes occurring at distances greater than 5 km, such as within the northwest cluster (Fig. 11c).

Two hypotheses for triggering of the northwest-cluster seismicity have been proposed previously. Roeloffs and Denlinger (2009) suggested that seismicity was initially triggered in the northwest cluster by stress redistribution. This hypothesis stems from the fact that the seismicity in the northwest cluster began only one year after the start of long-term injection operations, too soon for significant pore pressure changes to have propagated 6–8 km from the well, based on results from their axisymmetric porous-medium fluid flow model. An alternative explanation for the early onset of the northwest-cluster seismicity was suggested by Ake *et al.* (2005): one or more northwest-trending faults allow for fluid flow, and relatively rapid propagation of pore pressure, from the vicinity of the injection well to the northwest cluster. The concept of northwest-trending relatively high-permeability fault zones acting as fluid and pore-pressure conduits is consistent with the mapped geology and the local stress field (Ake *et al.*, 2005). In this model, earthquakes occurring in the northwest cluster, such as the January 2013 event, are inferred to be induced primarily by pore pressure changes. The observed lack of correlation between the average injection pressures at the well and the rates and magnitudes of earthquakes occurring in the northwest cluster appears to contradict this model. Likewise, the lack of similarity between the near-well and northwest-cluster temporal seismicity patterns (as shown in Fig. 11) appears to be inconsistent. However, a possible explanation for this inconsistency is that the high-permeability pathways between the near-well area and northwest cluster are pressure sensitive. When pore pressures in the vicinity of the well increase to sufficiently high levels, the conduits for fluid flow and pore-pressure propagation to the northwest may open, and pore pressures may then increase relatively quickly in the northwest cluster. When pore pressures in the vicinity of the injection well fall to sufficiently low levels, the conduits may close and the pressures in the northwest cluster may then be rela-

tively isolated from further pressure reductions at or near the injection well.

The occurrence of the January 2013 M_L 4.4 earthquake, at a distance from the injection well nearly four times greater than the radial distances of previous PVU-induced earthquakes of comparable size, is part of a broader trend of recently changing seismicity patterns related to PVU fluid injection. Patterns of PVU-induced seismicity largely stabilized for a decade following a decrease in the injection flow rate by one-third in mid-2000. Since 2010, however, seismicity rates have increased in some areas, and seismicity has been detected in previously aseismic areas. (Improved event detection capability does not account for most of the observed changes.) For example, seismicity rates in the southeast cluster increased from 3 events prior to 2010 to 53 events from 2010 to 2012. Seismicity rates within the northern-valley areas have also changed in recent years. The number of northern-valley earthquakes recorded each year from 2000 (when the northern valley seismicity was first detected) to 2009 ranges from 2 to 33. In 2010, the rate increased markedly: 557 northern-valley earthquakes were recorded, with the majority occurring in a single swarm lasting just 16 days. Northern-valley seismicity rates remained elevated during 2011, with 113 earthquakes recorded, but declined back to pre-2010 rates during 2012, with just 10 events recorded. Between 2010 and 2012, 10 shallow earthquakes were detected beneath central Paradox Valley. Although the total number of events is small, no earthquakes were detected within the valley in the 25 years of seismic monitoring prior to 2010. The renewed spatial expansion of seismicity and increased seismicity rates in recent years may be related to the trend of increasing injection pressures at the well.

The January 2013 earthquake did not occur on any of the subsurface faults that were mapped with seismic reflection surveys during early PVU geophysical investigations. Most of these faults trend close to the estimated direction of maximum horizontal stress (Ake *et al.*, 2005), and therefore they are not optimally oriented for shear slip. Most of the induced earthquakes observed at PVU, including the January 2013 event, appear to occur on unmapped faults, which were aseismic during the pre-injection period of monitoring. Because these faults may not have significant vertical offset, they may be difficult to resolve on deep seismic reflection data.

CONCLUSIONS

Our analyses indicate that the widely felt earthquake that occurred on 24 January 2013 (UTC) near the town of Paradox, Colorado, was induced by long-term fluid injection at the PVU, a salinity control facility operated by the Bureau of Reclamation. The earthquake occurred within a cluster of induced seismicity that has been active since mid-1997, approximately one year after the start of long-term PVU fluid injection, and appears to represent the full rupture of a fault segment delineated by the earlier seismicity. The 4.4 km depth of the earthquake is consistent with the depths of previously induced events and with the depth range of injection target formations.

The focal mechanism of the January 2013 earthquake and pattern of aftershocks indicate shear slip on an east-north-east-trending strike-slip fault, similar to mechanisms computed for many other PVU-induced earthquakes and consistent with a model of shear failure on a pre-existing fracture surface due to a decrease in the effective normal stress. The January 2013 event, with an estimated local magnitude of M_L 4.4, was slightly larger than the PVU-induced M_L 4.3 earthquake of 27 May 2000, making it the largest PVU-induced event to date. At a radial distance of 8.2 km from the injection well, the January 2013 earthquake occurred nearly four times farther from the well than any previous PVU-induced earthquake of comparable magnitude. The earthquake produced unusually large ground motions in the northern Paradox Valley area, with a peak horizontal acceleration of $0.29g$ recorded in the town of Paradox. 

ACKNOWLEDGMENTS

This paper summarizes studies done in support of the Paradox Valley Unit (PVU) following the 24 January 2013 earthquake. We thank Andy Nicholas, Tyler Artichoker, and Ed Warner for their support of PVU seismic monitoring and analysis. We thank the anonymous reviewers of this article for their helpful and constructive comments.

REFERENCES

Abrahamson, N., and W. Silva (2008). Summary of the Abrahamson & Silva NGA ground-motion relations, *Earthq. Spectra* **24**, no. 1, 67–97.

Ake, J., K. Mahrer, D. O’Connell, and L. Block (2005). Deep-injection and closely monitored induced seismicity at Paradox Valley, Colorado, *Bull. Seismol. Soc. Am.* **95**, no. 2, 664–683.

Block, L., and C. Wood (2009). *Overview of PVU-Induced Seismicity from 1996 to 2009 and Implications for Future Injection Operations*, Technical Memorandum No. 86-68330-2009-22, Bureau of Reclamation, Denver, Colorado, 16 pp.

Block, L. V., and C. K. Wood (2010). Evolving characteristics of seismicity induced by long-term fluid injection at Paradox Valley, Colorado, in *Abstract S13B–2000 presented at 2010 Fall Meeting*, AGU, San Francisco, California, 13–17 December.

Block, L., W. Yeck, V. King, S. Derouin, and C. Wood (2012). *Review of Geologic Investigations and Injection Well Site Selection, Paradox Valley Unit, Colorado*, Technical Memorandum No. 86-68330-2012-27, Bureau of Reclamation, Denver, Colorado, 62 pp.

Boore, D. M., and G. M. Atkinson (2008). Ground-motion prediction equations for the average horizontal component of PGA, PGV, and 5%-damped PSA at spectral periods between 0.01 s and 10.0 s, *Earthq. Spectra* **24**, no. 1, 99–138.

Bremkamp, W., and C. L. Harr (1988). Area of least resistance to fluid movement and pressure rise, *Report to the Bureau of Reclamation*, 49 pp.

Brune, J. N. (1970). Tectonic stress and the spectra of seismic shear waves from earthquakes, *J. Geophys. Res.* **75**, no. 26, 4997–5009.

Brune, J. N. (1971). Correction [to “Tectonic stress and the spectra, of seismic shear waves from earthquakes”], *J. Geophys. Res.* **76**, no. 20, 5002–5002.

Campbell, K. W., and Y. Bozorgnia (1987). *Campbell-Bozorgnia NGA Ground Motion Relations for the Geometric Mean Horizontal Component of Peak and Spectral Ground Motion Parameters*, Pacific

Earthquake Engineering Research Center, University of California, Berkeley.

Campbell, K. W., and Y. Bozorgnia (2008). NGA ground motion model for the geometric mean horizontal component of PGA, PGV, PGD and 5% damped linear elastic response spectra for periods ranging from 0.01 to 10 s, *Earthq. Spectra* **24**, no. 1, 139–171.

Cater, F. W. (1970). Geology of the salt anticline region in southwestern Colorado, *U.S. Geol. Surv. Prof. Pap.* **637**, U. S. Dept. of the Interior, Washington, D. C., 75 pp.

Chiou, B. S. J., and R. R. Youngs (2008). An NGA model for the average horizontal component of peak ground motion and response spectra, *Earthq. Spectra* **24**, no. 1, 173–215.

Garagash, D. I., and L. N. Germanovich (2012). Nucleation and arrest of dynamic slip on a pressurized fault, *J. Geophys. Res.* **117**, no. B10, 27 pp.

Gutierrez, F. (2004). Origin of the Salt Valleys in the Canyonlands section of the Colorado Plateau—Evaporite-dissolution Collapse versus tectonic subsidence, *Geomorphology* **57**, 423–435.

Jaeger, J. C. (1969). *Elasticity, Fracture, and Flow with Engineering and Geological Applications*, Chapman & Hall, London, 166 pp.

Kaklamanos, J., L. G. Baise, and D. M. Boore (2011). Estimating unknown input parameters when implementing the NGA ground-motion prediction equations in engineering practice, *Earthq. Spectra* **27**, no. 4, 1219–1235.

Kanamori, H., and D. L. Anderson (1975). Theoretical basis of some empirical relations in seismology, *Bull. Seismol. Soc. Am.* **65**, no. 5, 1073–1095.

King, V., L. Block, W. Yeck, C. Wood, and S. Derouin. Geological structure of the Paradox Valley Region, Colorado, and relationship to seismicity induced by deep well injection, *J. Geophys. Res.* (submitted).

Mahrer, K., J. Ake, L. Block, D. O’Connell, and J. Bundy (2005). Injecting Brine and inducing seismicity at the world’s deepest injection well, Paradox Valley, Southwest Colorado, in *Underground Injection Science and Technology*, Chin-Fu Tsang and John A. Apps (Editors), Elsevier B. V., Amsterdam, 361–376.

Power, M., B. Chiou, N. Abrahamson, Y. Bozorgnia, T. Shantz, and C. Roblee (2008). An overview of the NGA project, *Earthq. Spectra* **24**, no. 1, 3–21.

Roeloffs, E., and R. Denlinger (2009). An axisymmetric coupled flow and deformation model for pore pressure caused by brine injection in Paradox valley, Colorado: Implications for the mechanisms of induced seismicity, *Preliminary Report to the Bureau of Reclamation*, *U.S. Geol. Surv.*, 31 pp.

Shapiro, S. A., O. S. Krüger, C. Dinske, and C. Langenbruch (2011). Magnitudes of induced earthquakes and geometric scales of fluid-stimulated rock volumes, *Geophysics* **76**, no. 6, WC55–WC63.

Silkman, B. (2013). Bedrock earthquake jolts all the way to the Grand Valley; available from <http://www.kjct8.com/news/Bedrock-Earthquake-jolts-all-the-way-to-the-Grand-Valley/-/163152/18271974/-/e07pyaz/-/index.html> (retrieved 25 September 2013).

Trudgill, B. D. (2011). Evolution of salt structures in the northern Paradox Basin: Controls on evaporite deposition, salt wall growth and supra-salt stratigraphic architecture, *Basin Res.* **23**, no. 2, 208–238.

Lisa V. Block
Christopher K. Wood
William L. Yeck
Vanessa M. King
Bureau of Reclamation
P.O. Box 25007
Mail Code 86-68330
Denver, Colorado 80225 U.S.A.
lblock@usbr.gov